Polar Geosci , **13**, 86-102, 2000

LREE-enriched mafic gneiss and meta-ultramafic rock from Tonagh Island in the Napier Complex, East Antarctica

Masaaki Owada[1], Yasuhito Osanai[2], Toshiaki Tsunogae[3], Tsuyoshi Toyoshima[4], Tomokazu Hokada[5] and Warwick A Crowe[6]

[1]*Department of Earth Sciences, Yamaguchi University, Yoshida 1677-1, Yamaguchi 753-8512, e-mail. owada@sci yamaguchi-u ac jp*
[2]*Department of Earth Sciences, Okayama University, Tsushima-naka 3-1-1, Okayama 700-8530*
[3]*Department of Earth Sciences, Shimane University, Nishi Kawazu, Matsue 690-8504*
[4]*Graduate School of Science and Technology, Niigata University, Ikarashi 2-chome, Niigata 950-2181*
[5]*National Institute Polar Research, Kaga 1-chome, Itabashi-Ku, Tokyo 173-8515*
[6]*Department of Geology and Geophysics, University of Western Australia, Nedlands, Perth, WA 9607, Australia*

Abstract: Mafic gneisses and meta-ultramafic rocks are exposed on Tonagh Island These rocks are high-Mg composition and have undergone ultrahigh-temperature metamorphism Most of the mafic gneisses and the meta-ultramafic rocks occur as intercalated layers or lenses within the quartzo-feldspathic gneisses Some of the mafic gneisses and the meta-ultramafic rocks locally cut the layers or foliations of neighboring quartzo-feldspathic gneisses, suggesting that these mafic gneisses and meta-ultramafic rocks were originally intrusive rocks Major and trace element compositions of the mafic gneisses and the meta-ultramafic rocks resemble those of komatiitic basalt to komatiite from the Archaean greenstone belt Light REE-enriched and flat patterns are recognized in the mafic gneisses and meta-ultramafic rocks although the REE pattern of the deformed sample is convex upward In the Mt Riiser-Larsen region situated 40 km northeast from Tonagh Island, it has been found in a previous study that the LREE-enriched mafic gneisses and meta-ultramafic rocks have been derived from komatiitic rocks whose chemical trends show magmatic variations Therefore, the LREE-enriched patterns of mafic gneisses and ultramafic rocks on Tonagh Island and in the Mt Riiser-Larsen region could be inherited from the chemical nature of original rocks prior to undergoing ultrahigh-temperature metamorphism The LREE-enriched pattern cannot be explained by interaction between an LREE-flat parental magma and an LREE-enriched crustal material in terms of geochemical constraints Hence, the LREE-enriched and flat types of the mafic gneisses and the meta-ultramafic rocks on Tonagh Island would have been derived from different source mantles with respect to LREE signatures

key words Archaean, Napier Complex, mafic gneiss and meta-ultramafic rock, REE geochemistry, source mantle

1. Introduction

The Napier Complex, East Antarctica is one of the oldest Archaean complexes in the world. It is also recognized as metamorphic terrane having undergone ultrahigh-temperature (UHT) metamorphism, characterized by spinel-quartz, sapphirine-quartz and orthopyroxene-sillimanite-quartz associations (*e.g* Sheraton *et al*, 1980, 1987) Metamorphic P-T conditions are up to 1 1 GPa and 1100°C (*e.g* Harley and Hensen, 1990) The dominant rock type is pyroxene- and garnet-bearing quartzo-feldspathic gneiss of igneous origin (orthogneiss), with subordinate mafic, ultramafic and sedimentary rocks (Sheraton *et al*, 1980, 1987). The tonalitic precursor of the orthogneiss intruded into the crust *c.* 3900–3800 Ma, as revealed by ion microprobe U-Pb analysis of zircon (Black *et al*, 1986, Harley and Black, 1997). Granitic intrusive rocks and mafic dykes are also present (Sheraton and Black, 1981).

Geochemical studies for the mafic gneisses and meta-ultramafic rocks from the Napier Complex have been conducted by previous workers (*e.g* Sheraton and Black, 1981, Sheraton *et al*, 1987, Owada *et al*, 1995, Tainosho *et al*, 1997, Owada *et al*, 1999, Suzuki *et al*, 1999) Sheraton *et al*. (1987) revealed that some mafic gneisses from the Napier Complex are similar geochemical features to Archaean komatiitic rock Tainosho *et al* (1997) noted that the mafic gneisses come from different source material from that of the quartzo-felspathic gneisses Suzuki *et al* (1999) argued that various kinds of original rocks are intermingled in the Mt Riiser-Larsen region in terms of the geochemical constraints They also revealed that the protolith of the phlogopite-bearing meta-ultramafic rock was derived from a komatiitic rock Furthermore, they implied that the quartz-bearing mafic gneiss probably represented a differentiated magma from a komatiite magma Chondrite normalized REE patterns of both the phlogopite-bearing meta-ultramafic rock and the quartz-bearing mafic gneiss are LREE-enriched. The hornblende-bearing meta-ultramafic dyke on Tonagh Island has LREE-enriched composition (Owada *et al*, 1999). Owada *et al* (1999) indicated that the protolith of this meta-ultramafic rock had similar petrological characteristics with a komatiitic rock from the Archaean greenstone belt

As described above, both LREE-enriched patterns of mafic gneisses and meta-ultramafic rocks are present in the Napier Complex In this paper, we describe the petrography and geochemistry of the mafic gneisses and meta-ultramafic rocks from Tonagh Island, with discussion of the geochemical nature of the precursor of the mafic gneisses and the ultramafic rocks.

2. Outline of geology

Tonagh Island is located in the southern part of Amundsen Bay The island consists of various kinds of metamorphic rocks, *e.g* orthopyroxene- and/or garnet-bearing quartzo-feldspathic gneiss, mafic gneiss, pelitic gneiss and ultramafic rock, and subordinate amounts of three types of unmetamorphosed intrusive rocks (dolerite, granitic pegmatite and syenite). The island is divided into five geological units (Unit I to V) from north to south (Fig. 1) These units are divided from each other by NE-SW to E-W striking and steeply north dipping shear zones. The dolerite dyke, named Amundsen dyke, cuts the host

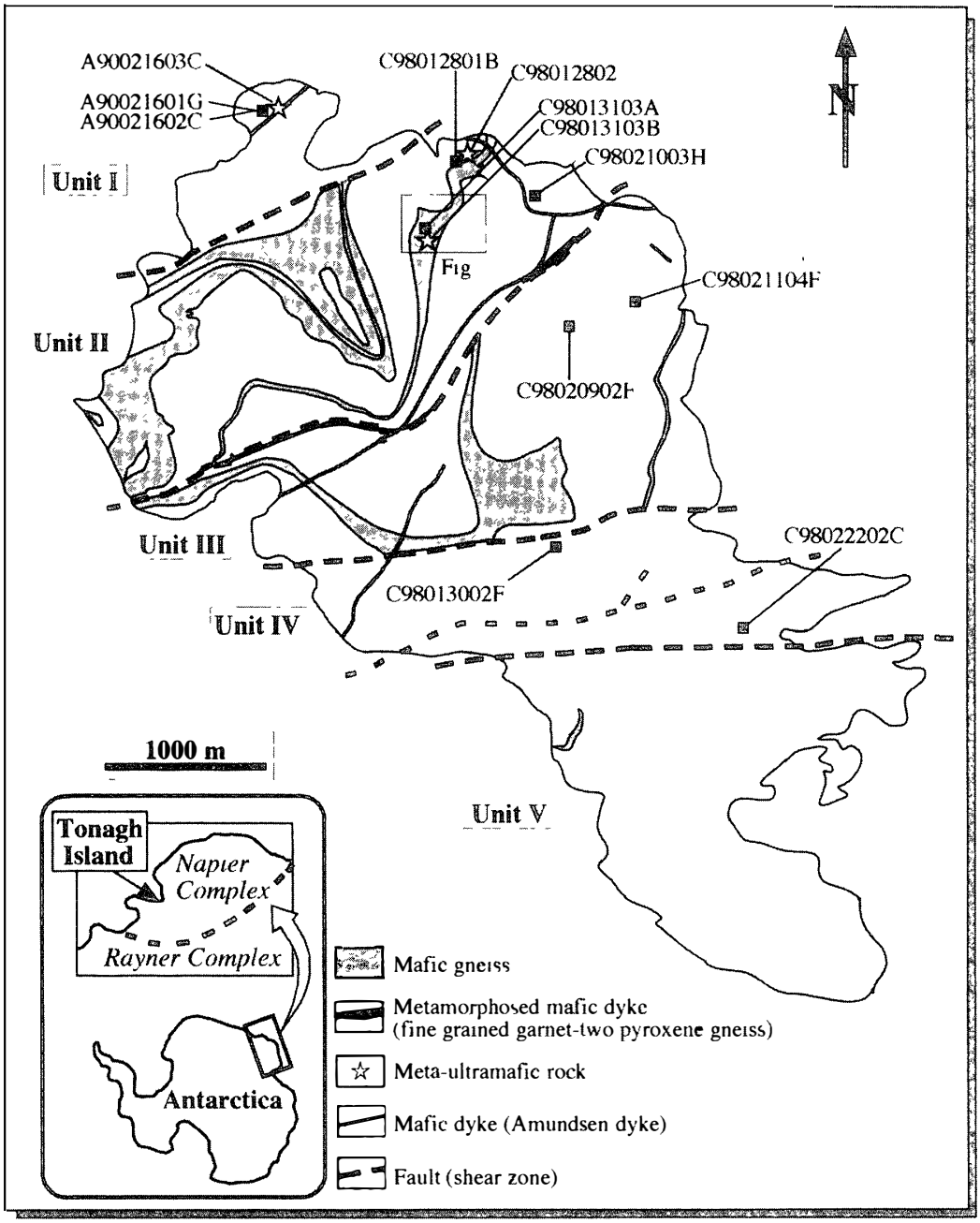

Fig 1 Location map of Tonagh Island with distribution of thick mafic gneiss layers and sample localities of analytical samples Units I to V denote lithological units separated by shear zones after Osanai et al (1999)

gneisses and the shear zone, and has a chilled margin Osanai *et al* (1999) and Toyoshima *et al* (1999) described lithological and structural features of each Unit Hokada *et al* (1999) discussed metamorphism of sapphirine-bearing aluminous gneiss from Tonagh Island and calculated metamorphic P-T conditions by geothermobarometries According to them, inferred P-T conditions using mineral chemistries are 800–1000°C and 0 8–1 1 GPa

Unit I is composed of layered gneiss, which is combination of following rock types

on a scale of 1–20 m in thickness the orthopyroxene- and garnet-bearing quartzo-feldspathic gneiss, the mafic gneiss, the pelitic gneiss and the quartz-magnetite gneiss Minor meta-ultramafic rocks occur as thin layers or lenses within the mafic, the quartzo-feldspathic and the pelitic gneisses Units II and III are characterized by the presence of the thick mafic gneiss layers (Fig 1) The hornblende-bearing lherzolitic peridotite cutting the layered structure of the host gneiss appears in Unit II (Owada *et al*, 1999) In addition to these rocks, garnet two pyroxene mafic dyke intruded into the boundary between Units II and III (Fig 1) Unit IV consists mainly of layered gneiss, which is underlain by a narrow zone between Units III and V The quartzo-feldspathic gneiss in Unit IV strongly underwent mylonitic deformation, although the mafic gneiss does not show apparent deformation Unit V contains widely distributed orthopyroxene-bearing quartzo-feldspathic gneiss with trace amounts of the mafic, pelitic gneisses and quartz-magnetite gneiss Meta-ultramafic rocks are sporadically observed as small lenses and blocks through the whole unit The foliation in Unit I strikes NE-SW and dips SE or NW with a steep angle (50–80°C) These in Units II and III show almost the same trend as those in Unit I, but dip gently (15–40°) NW In Units IV and V, the foliation strikes NE-SW and dips north with moderate angle (20–60°)

3. Occurrence and petrography of samples

Lithologies of the mafic gneisses and the meta-ultramafic rocks are classified into the following eight types (Owada *et al*, 1999) 1) two pyroxene gneiss, 2) garnet-bearing two pyroxene gneiss, 3) brown hornblende two pyroxene gneiss, 4) biotite-bearing two pyroxene gneiss, 5) fine grained garnet two pyroxene gneiss, 6) pyroxenite, 7) websteritic peridotite, and 8) hornblende-bearing lherzolitic peridotite Analytical samples used for this study are chosen from 1), 3), 4), 7) and 8) Mineral assemblages and sample localities are given in Table 1 and Fig 1, respectively. Lithological names of the mafic gneisses are abbreviated by Px mafic gneiss for the two pyroxene gneiss, Hbl mafic gneiss for the brown hornblende two pyroxene gneiss and Bt mafic gneiss for the biotite-bearing two pyroxene mafic gneiss The hornblende-bearing lherzolitic peridotite refers to Hbl lherzolitic peridotite Texture and metamorphic reactions of the mafic gneisses are described by Tsunogae *et al* (1999)

3.1. Px mafic gneiss

The Px mafic gneiss crops out in each unit This gneiss is observed as both thick and thin layers The Px mafic gneiss is medium-grained and shows granoblastic texture Apatite and Fe-Ti oxide minerals are observed as accessory minerals Retrograde green hornblende and biotite are present (Tsunogae *et al*, 1999; Owada *et al*, 1999) Sample C98022202C is exposed on the shear zone in Unit V (Fig 1) This sample shows mylonitic deformation (Fig 2)

3.2. Hbl mafic gneiss

The Hbl mafic gneiss occurs as thick layers in Units I and II (Fig 1) Compositional banding associated with the meta-ultramafic layer locally develops in the mafic layer (Fig 3) This gneiss is characterized by the presence of coarse-grained brown hornblende

Table 1 Approximate modal abundance of minerals in the mafic gneisses and the meta-ultramafic rocks from Tonagh Island Mineral abbreviations are after Kretz (1983)

Sample No.	Unit	Occurrence	Ol	Cpx	Opx	Hbl	Grt	Bt	Pl	Qtz	Spl	Ap
Mafic gneiss												
A90021601G	Unit I	layer		○	○	△		△	○			×
A90021602C	Unit I	layer		○	○	△		△	○			×
C98012801B	Unit II	layer		○	○	○			○			×
C98013103A	Unit II	layer		○	○	○			○		△	
C98021003H	Unit II	layer		○	○			△	○	△		×
C98020902F	Unit III	layer		○	○			△	○	△		×
C98021104F	Unit III	layer		○	○			○	○	△		×
C98013002F	Unit IV	layer		○	○		○	○	○		△	
C98022202C	Unit V	layer		○	○		△	△	○	△		×
Meta-ultramafic rock												
C98012802	Unit II	dyke	○	○	○	○					△	×
A90021603C	Unit I	layer		○	○	△		△	△			×
C98013103B	Unit II	lens	△	○	○	○			△		△	

○: common, △: rare, ×: accessory

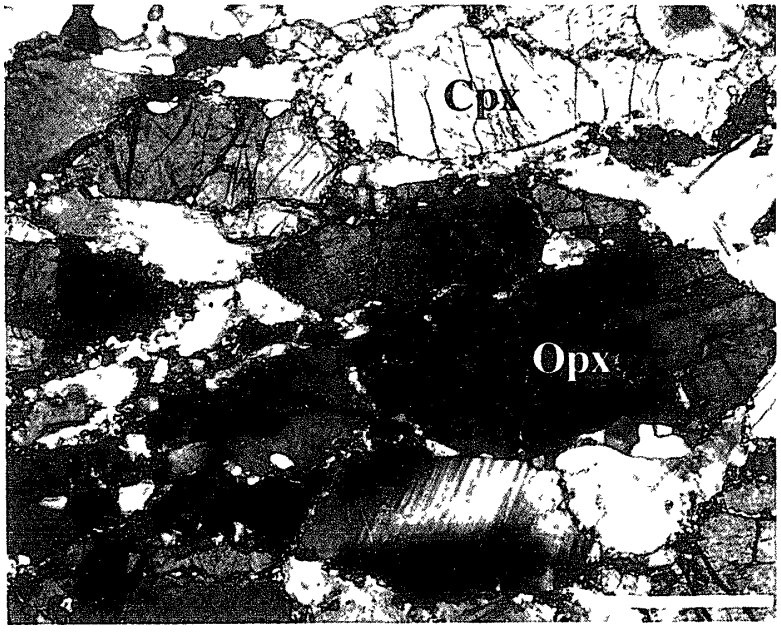

Fig 2 Photomicrograph of the Px mafic gneiss (sample C98022202C) Scale bar is 0 5 mm Note that this sample shows mylonitic deformation Abbreviations are the same as Table 1

coexisting with pyroxene and plagioclase (Table 1) The Hbl mafic gneiss contains apatite and Fe-Ti oxide minerals as accessory minerals Petrographical feature indicates that the brown hornblende was present at the peak metamorphic condition coexisting with

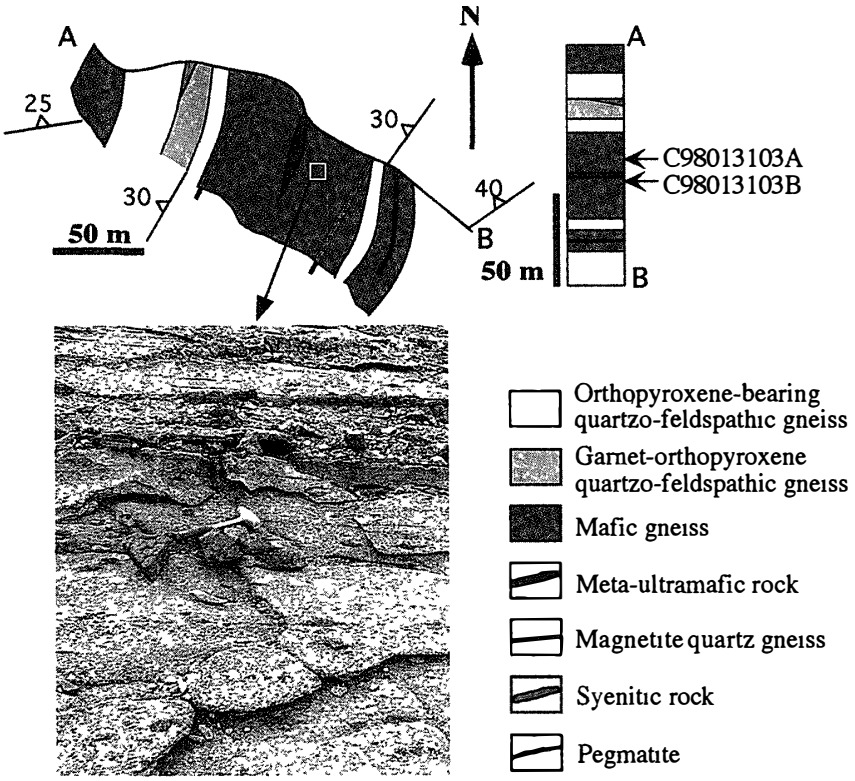

Fig. 3 Route map showing the relationship among the quartzo-feldspathic gneiss, the mafic gneiss and the meta-ultramafic rock in Unit II, with sampling localities Note that the Hbl mafic gneiss shows compositional banding and the association with thin layers of websteritic peridotite

pyroxene and plagioclase (Owada *et al*, 1999)

3.3. Bt mafic gneiss

The Bt mafic gneiss is observed in the layered gneiss from Units III and IV This gneiss is dark brown to grayish brown in color because of large amounts of reddish brown biotite Sample C98013002F is present as a lens in the strongly mylonitized quartzo-feldspathic gneiss in Unit IV Small amounts of garnet surround pyroxene and coexist with biotite (Fig 4a) Sample C98021104F occurs as a thin layer within the quartzo-feldspathic gneiss and is characterized by large amounts of biotite Symplectite of biotite and quartz is frequently observed (Fig 4b). A quartz vein penetrates into the sample The Bt mafic gneiss contains apatite and Fe-Ti oxide minerals as accessory minerals. Zircon is also present as inclusions in biotite

3.4. Websteritic peridotite

The websteritic peridotite occurs as a lens or a block. The peridotite consists mainly of orthopyroxene, clinopyroxene and a small amount of olivine Brown to brownish green spinel, phlogopite, brown to pale brown hornblende and plagioclase are also present as primary minerals Euhedral apatite is observed in the layered type websteritic peridotite as an inclusion of plagioclase and pyroxene Sample C98013103B occurs as a thin lens within the thick Hbl mafic gneiss layer in Unit II (Figs 1 and 3) Sample C98013103B

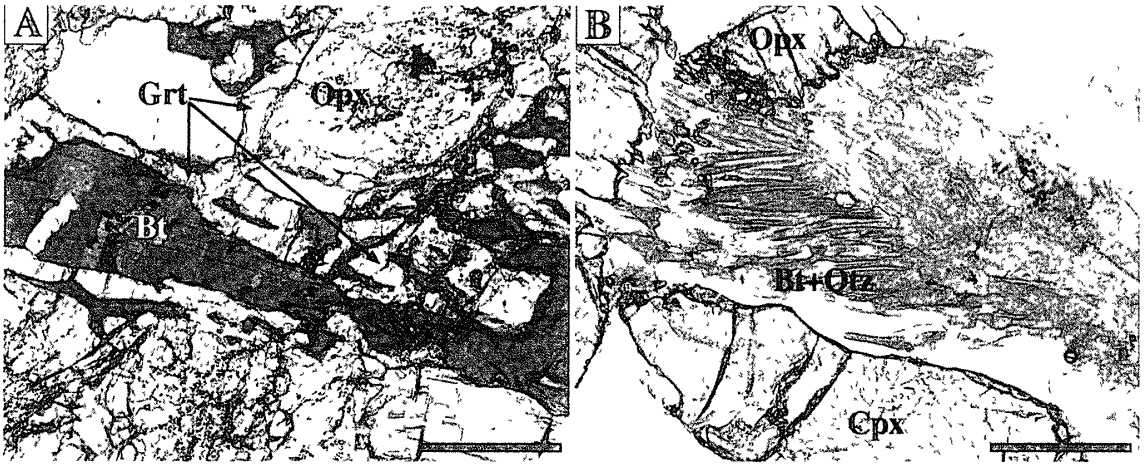

Fig 4 Photomicrographs of the Bt mafic gneiss Scale bars are 0 25 mm A sample C98013002F Note that this sample contains a large amount of biotite coexisting with garnet B sample C98021104F Note that biotite and quartz symplectite is frequently observed Mineral abbreviations are the same as Table 1

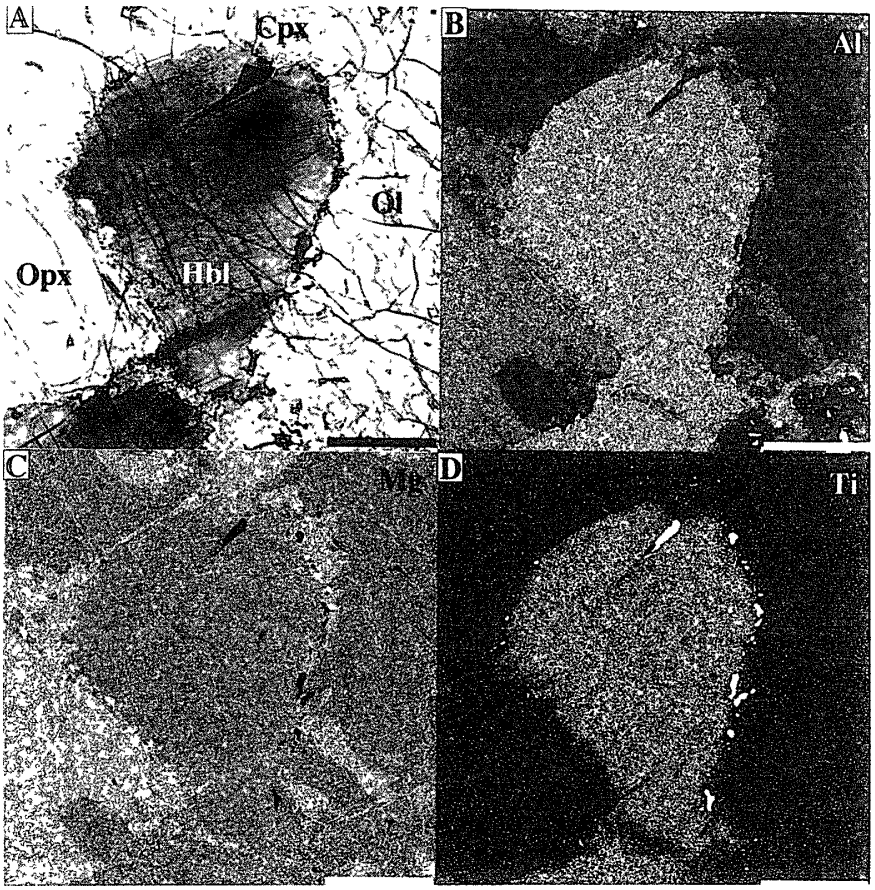

Fig 5 Photomicrograph and compositional map of constituent minerals in the Hbl lherzolitic peridotite (sample C98012802) All scale bars are 0 5 mm A warm color represents higher-concentration and a cold one is lower-concentration of each element Note that constituent minerals do not show chemical zoning A Photomicrograph of the sample B X-ray map of Mg C X-ray map of Al D X-ray map of Ti Mineral abbreviations are the same as Table 1

and the Hbl mafic gneiss (sample C98013103A) are similar mineral assemblages but have different modal compositions (Table 1).

3.5. Hbl lherzolitic peridotite

The Hbl lherzolitic peridotite is oblique against the layers of the neighboring quartzo-feldspathic gneiss, suggesting that this rock was intrusive rock (Owada *et al*., 1999) It shows granoblastic texture and consists mainly of olivine, clinopyroxene, orthopyroxene and hornblende (Fig 5), with trace amounts of spinel, magnetite and apatite Euhedral to subhedral apatite is included in olivine (Owada *et al*., 1999) Figure 5 shows results of compositional mapping of Al, Mg and Ti Chemical compositions of constituent minerals such as olivine, pyroxene and hornblende are homogeneous Representative pyroxene compositions are listed in Appendix 1 Judging from texture combined with mineral chemistry, these minerals probably reached equilibrium during peak metamorphism

4. Bulk rock chemistry

Major and some minor elements were analyzed with XRF at the Center of Instrumental Analysis of Yamaguchi University Trace elements including rare earth elements (REE) were determined by Inductively Coupled Plasma Mass spectrometry (ICP-MS) at Activation Laboratory Co Ltd and the Curtin University of Technology The analytical data are listed in Table 2

The mafic gneisses and the meta-ultramafic rocks range from 43 to 55 wt% in SiO_2 Some of these rocks are characterized by high MgO, Cr and Ni contents Figure 6 shows the Ti (ppm)-Zr (ppm) diagram of the rocks from Tonagh Island and komatiitic rocks from Barberton greenstone belt All samples are plotted close to the primitive mantle composition described by Sun and McDonough (1989)

Chondrite normalized REE patterns for the mafic gneisses and the meta-ultramafic rocks are given in Fig 7 The REE patterns of the Hbl mafic gneiss show enrichment in LREE and slight depletion in HREE, although sample A90021602C shows relative HREE depletion compared with the other three samples Sample C98013103A, which has the lowest REE abundance among the Hbl mafic gneiss, was collected from the central part of a thick mafic layer in Unit II (Fig 3) The other three gneisses occur as relatively thick layers in Units I and II The patterns of these samples resemble each other (Fig 7)

The REE patterns of the Px mafic gneiss are similar to those of the Hbl mafic gneiss except for sample C98022202C The REE pattern of this sample is a convex upward and is different from those of other mafic gneisses and meta-ultramafic rocks (Fig 7) The REE pattern of the sample was probably modified during deformation since the sample underwent mylonitic deformation (Fig 2)

Two samples of the Bt mafic gneiss were measured Sample C98021104F shows an LREE-enriched pattern, whereas sample C98013002F shows an almost flat pattern although HREE concentrations are similar

The REE patterns of the meta-ultramafic rocks are divided into two types, LREE-enriched and flat types (Fig 7). Both types have similar HREE compositions Sample C98013103B is present in the thick mafic layer of the Hbl mafic gneiss, and was collected

Table 2 Bulk rock analyses of the mafic gneisses and the meta-ultramafic rocks from Tonagh Island

Sample No	A90021601G	A90021602C	C98012801B	C98013103A	C98021003H	C98020902F	C98021104F	C98013002F	C98022202C	A90021603C	C98013103B	C98012802
Unit	Unit I	Unit I	Unit II	Unit II	Unit II	Unit III	Unit III	Unit IV	Unit V	Unit I	Unit II	dyke
Rock type	BHPG	BHPG	BHPG	BHPG	PG	PG	BPG	BPG	PG	WP	WP	HLP
wt %												
SiO_2	54 82	50 36	50 48	47 06	50 46	52 70	54 50	45 07	49 84	53 30	42 33	43 95
TiO_2	0 45	1 11	0 92	0 41	0 62	0 75	0 59	0 98	0 69	0 33	0 37	0 51
Al_2O_3	12 86	8 72	16 08	19 14	12 89	14 56	9 76	15 09	15 31	3 49	10 58	4 30
Fe_2O_3	10 59	15 03	10 42	9 30	12 74	12 29	11 15	15 27	12 44	12 24	15 16	15 14
MnO	0 17	0 23	0 14	0 12	0 22	0 17	0 14	0 23	0 23	0 21	0 20	0 20
MgO	10 51	14 76	8 82	11 40	9 35	8 55	13 95	11 87	7 82	23 71	23 22	31 05
CaO	8 87	8 10	11 35	11 18	12 22	7 42	5 81	9 51	14 49	6 84	6 19	4 97
Na_2O	2 03	1 17	2 36	1 48	1 92	3 05	1 93	0 53	0 67	0 32	0 51	0 36
K_2O	0 40	1 03	0 31	0 17	0 22	0 53	1 50	1 38	0 13	0 00	0 17	0 06
P_2O_5	0 08	0 26	0 12	0 02	0 05	0 07	0 30	0 06	0 12	0 04	0 03	0 02
ppm												
V	217	157	210	103*	239	209	143	286	218	124	149*	199*
Cr	736	1800	505	247*	1190	623	1170	286	607	5170	1139*	2142*
Co	48	76	55	nd	53	46	43	56	48	96	nd	nd
Ni	198	680	234	372*	121	95	143	131	102	676	1147*	1786*
Cu	16	51	73	nd	19	29	<10	59	<10	62	nd	nd
Zn	94	91	60	63*	106	122	74	82	82	123	146*	87*
Ga	15	15	17	nd	15	16	14	16	17	7	nd	nd
Rb	10	36	2	<2*	5	4	124	25	2	<2	<2*	6*
Sr	69	120	152	130*	57	108	240	61	103	5	20*	36*
Y	20	27	36	10	30	32	22	18	45	11	13	12
Zr	86	108	75	25	61	81	126	40	35	36	39	48
Nb	2 9	4 7	4 3	1 3	4 8	6 3	4 5	2 3	4 0	0 8	2 0	8 6
Ba	61	259	91	39	46	175	828	165	23	9	18	4

La	10 90	17 30	13 40	2 95	12 90	22 60	28 40	3 17	7 79	6 19	1 72	5 35
Ce	23 30	37 40	29 00	6 44	31 20	43 20	58 30	8 00	24 50	15 60	5 16	13 74
Pr	2 61	4 23	3 27	0 81	3 60	4 45	6 22	1 09	3 58	1 74	0 78	1 78
Nd	11 30	19 20	15 00	4 10	14 80	18 10	26 80	5 99	18 60	7 41	4 35	8 88
Sm	2 98	4 97	4 37	1 20	3 96	4 25	5 94	1 94	6 73	1 59	1 30	2 22
Eu	0 661	1 570	1 100	0 520	0 803	1 110	1 260	0 869	2 450	0 331	0 420	0 670
Gd	3 10	4 97	4 71	1 44	4 38	4 65	5 26	2 31	7 39	1 78	1 57	2 32
Tb	0 53	0 83	0 89	0 27	0 80	0 80	0 71	0 46	1 49	0 29	0 32	0 39
Dy	3 43	4 92	5 89	1 60	5 04	5 00	3 95	2 97	8 45	1 84	1 88	2 13
Ho	0 74	1 01	1 28	0 34	1 06	1 10	0 76	0 68	1 55	0 38	0 41	0 41
Er	2 15	2 75	3 79	0 91	3 15	3 44	2 18	2 06	4 01	1 15	1 16	1 06
Tm	0 318	0 384	0 574	0 140	0 471	0 541	0 309	0 330	0 541	0 178	0 190	0 160
Yb	1 98	2 23	3 35	0 95	2 69	3 25	1 87	1 97	2 92	1 01	1 32	0 99
Lu	0 273	0 337	0 466	0 150	0 386	0 477	0 246	0 299	0 322	0 151	0 220	0 150
Hf	2 2	3 0	1 8	0 7	1 7	2 3	3 1	1 2	1 3	0 9	0 9	1 7
Ta	0 3	0 4	0 3	0 2	0 5	0 7	0 4	0 2	0 5	0 1	0 3	1 0
Th	0 73	1 92	3 62	0 01	5 89	2 21	4 67	0 16	1 08	1 13	0 11	1 53
U	0 30	0 52	0 76	0 00	1 30	0 70	2 02	0 06	0 35	0 36	0 02	0 43
$(La/Yb)_N$	3 72	5 24	2 70	2 10	3 24	4 70	10 26	1 09	1 80	4 14	0 88	3 65
$(La/Sm)_N$	2 30	2 19	1 93	1 55	2 05	3 35	3 01	1 03	0 73	2 45	0 83	1 52

Total Fe as Fe_2O_3

Notes BHPG = brown hornblende two pyroxene gneiss (Hbl mafic gneiss), PG = two pyroxene gneiss (Px mafic gneiss), BPG = biotite-bearing two pyroxene gneiss (Bt mafic gneiss), WP = websteritic peridotite, HPL = hornblende-bearing lherzolitic peridotite (Hbl lherzolitic peridotite) * determined with XRF at Yamaguchi University

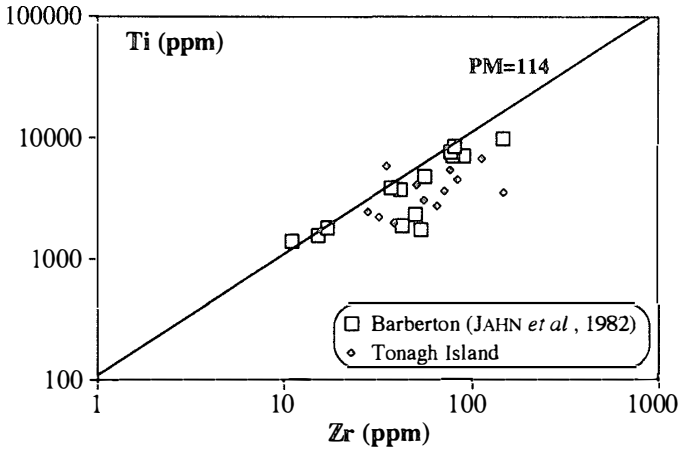

Fig 6 Ti (ppm)–Zr (ppm) diagram of the mafic gneisses and the meta-ultramafic rocks from Tonagh Island and komatiitic rocks from the Barberton greenstone belt, South Africa after Jahn et al (1982) PM primitive mantle values after Sun and McDonough (1989)

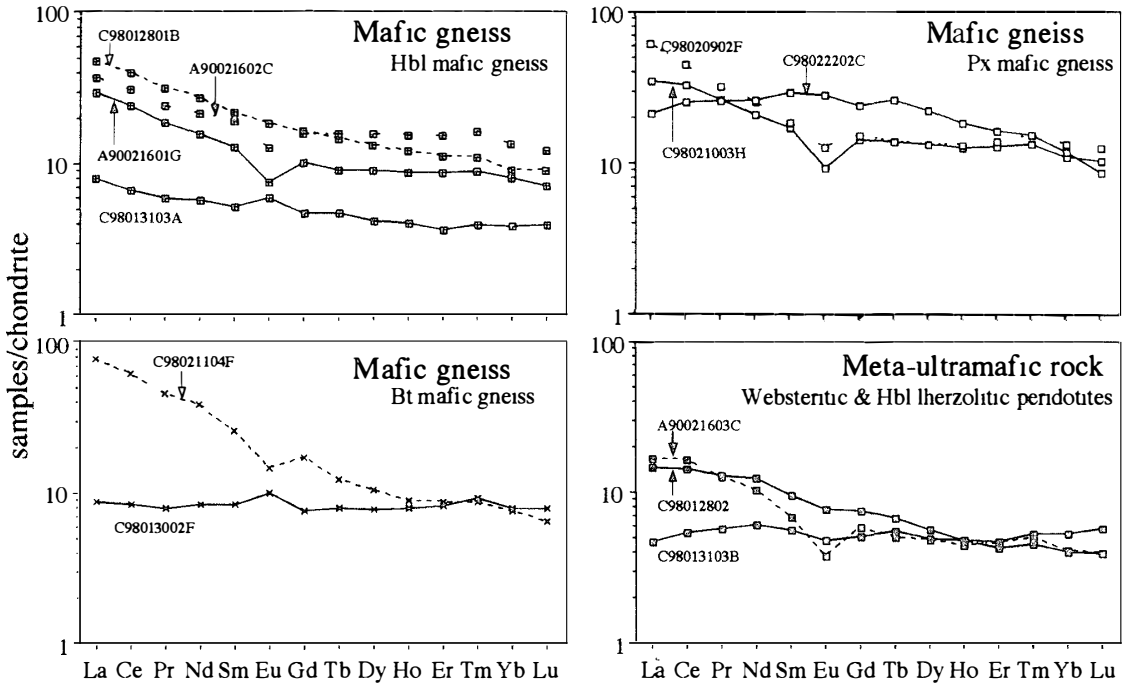

Fig 7 Chondrite normalized REE patterns of the mafic gneisses and the meta-ultramafic rocks from Tonagh Island

nearby the sample C98013103A (Fig 3) Both samples have low REE concentrations compared to other samples (Fig 7)

5. Discussion

Owada *et al* (1999) found that the precursor of the Hbl lherzolitic peridotite was intrusive rock based on geological and petrographical investigations Moreover, they

revealed that some original rocks of the mafic gneisses and the meta-ultramafic rocks had similar petrologic character to komatiitic rocks from the Archaean greenstone belt Figure 6 shows a Zr against Ti diagram for the mafic gneisses and the meta-ultramafic rocks from Tonagh Island and the komatiite and related basalt from the Barberton greenstone belt, South Africa. The Zr and Ti values of the mafic gneisses and meta-ultramafic rocks from Tonagh Island resemble those of the komatiitic rocks from Barberton greenstone belt The Ti and Zr data support the above idea proposed by Owada *et al* (1999)

The Hbl mafic gneiss is characterized by enrichment in LREE and slight depletion in HREE regardless of their REE concentrations Most of the Px mafic gneiss, the Bt mafic gneiss and the meta-ultramafic rocks represent an LREE-enriched pattern and are similar REE patterns to the Hbl mafic gneiss (Fig. 7) Sample C98021104F (the Bt mafic gneiss) shows distinct LREE enrichment between the mafic gneisses and the meta-ultramafic rocks (Fig 7) A large amount of biotite and quartz symplectite is recognized in the sample (Fig 4b) Tsunogae *et al*. (1999) described similar texture in other mafic gneisses from Tonagh Island They interpreted that this texture shows retrograde interaction between a mafic gneiss and a melt Taking their interpretation into account, the REE pattern of sample C98021104F is considered to have resulted from interaction between a mafic gneiss and a probably LREE-enriched melt, although the data presented here are insufficient to discuss the interaction process

Cattell (1987) found that LREE enrichment of komatiitic basalt from the late Archaean greenstone belt in Canada reflects a result of interaction between LREE depleted komatiitic magma and LREE-enriched crustal materials Figure 8 shows the chondrite normalized $(La/Yb)_N$-Yb_N diagram for the mafic gneisses and meta-ultramafic rocks from Tonagh Island and the orthopyroxene felsic gneiss from Mt Riiser-Larsen (data set from Suzuki *et al*, 1999) The mafic gneisses and the meta-ultramafic rocks, excluding sample C98021104F, show low $(La/Yb)_N$ ratios regardless of Yb concentration, whereas the orthopyroxene felsic gneisses plotted within the field of Archaean TTG represent high $(La/Yb)_N$ ratios and low Yb contents (Fig. 8) If a meta-ultramafic rock ($Yb_N = 13.5$, $(La/Yb)_N = 2.7$) is mixed with an orthopyroxene felsic gneiss as a contaminant ($Yb_N = 1.1$, $(La/Yb)_N = 104$), resulting compositions are plotted on the mixing line shown in Fig 8 Most of the mafic gneisses and meta-ultramafic rocks are not plotted on the line Therefore, the LREE-enriched patterns of most of the mafic gneisses and meta-ultramafic rocks cannot be explained by interaction between LREE depleted or flat parental mafic to ultramafic magmas and the LREE-enriched crustal orthopyroxene felsic gneisses

The LREE-enriched ultramafic rocks have been described by Suzuki *et al* (1999) in the Mt Riiser-Larsen region. They found that the phlogopite-bearing metaultramafic rock has been derived from komatiitic rocks, of which it shows a magmatic compositional variation controlled by addition and subtraction of olivine Therefore, geochemical data presented here combined with the interpretation of Suzuki *et al* (1999) suggests that the LREE-enriched pattern of these samples, excluding sample C98021104F, may reflect the chemical nature of original rocks before they underwent ultrahigh-temperature metamorphism

As already described, LREE-flat to slightly depleted mafic gneisses and ultramafic rocks are exposed on Tonagh Island and also occur in the Mt Riiser-Larsen region (Suzuki *et al*, 1999) According to the mineral/liquid partition coefficient for the tholeiitic

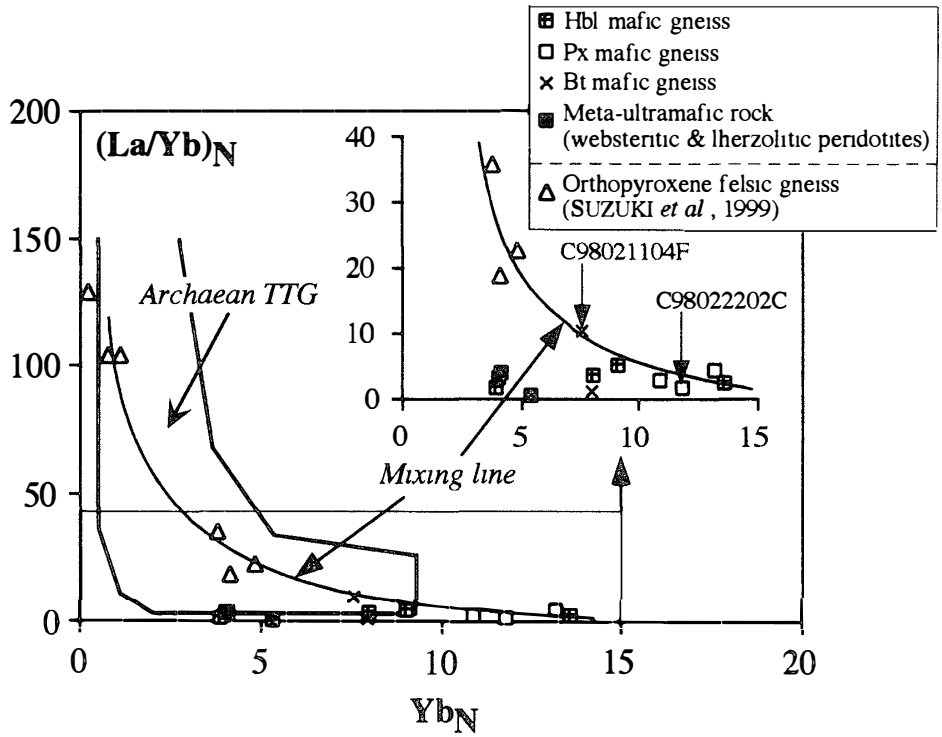

Fig 8 Chondrite normalized $(La/Yb)_N$-Yb_N diagram of the mafic gneisses and the meta-ultramafic rocks from Tonagh Island and the orthopyroxene felsic gneisses from the Riiser-Larsen region after Suzuki et al (1999) The solid line is the mixing line between assumed parental magma ($Yb_N = 13\ 5$ and $(La/Yb)_N = 2\ 7$) and crustal contaminant ($Yb_N = 1\ 1$ and $(La/Yb)_N = 104$). The Archaean TTG field is after Martin (1986)

system, a common fractionating assemblage such as olivine, clinopyroxene or plagioclase cannot alter results in LREE-enriched residual liquids from LREE flat to depleted parental magma (Sun and Nesbitt, 1978) It is known that the LREE enrichment could be ascribed to late-stage crystallization of zircon in the same system (Tribuzio *et al* , 2000) This situation cannot be applied in the mafic to ultramafic rocks because zircon crystallizes from highly evolved melt such as rhyolite Therefore, the LREE-enriched patterns cannot be explained by fractional crystallization of parental REE flat magma Suzuki *et al* (1999) found that their source mantles have different LREE signatures, namely, an LREE-enriched mantle for the quartz-bearing mafic gneiss and an LREE-depleted mantle for the quartz-free varieties

Owada *et al* (1999) pointed out that diversity of the LREE enrichment might reflect the modal abundance of apatite The variations of Ce (ppm)-P (ppm) concentration are given in Fig 9 These elements indicate positive correlation, suggesting that apatite is regarded as a main container of REE in the mafic gneisses and the meta-ultramafic rocks from Tonagh Island Figure 10 shows the chondrite normalized $(La/Yb)_N$ ratio against P_2O_5 (wt%) diagram of the mafic gneisses and the meta-ultramafic rocks LREE-enriched samples, excluding C98021104F, show positive correlation between $(La/Yb)_N$ ratios and P_2O_5 contents, suggesting that diversity of $(La/Yb)_N$ ratios roughly correlates with modal abundance of apatite In comparison with the same P_2O_5 contents ($>0\ 1$ wt%), LREE-flat

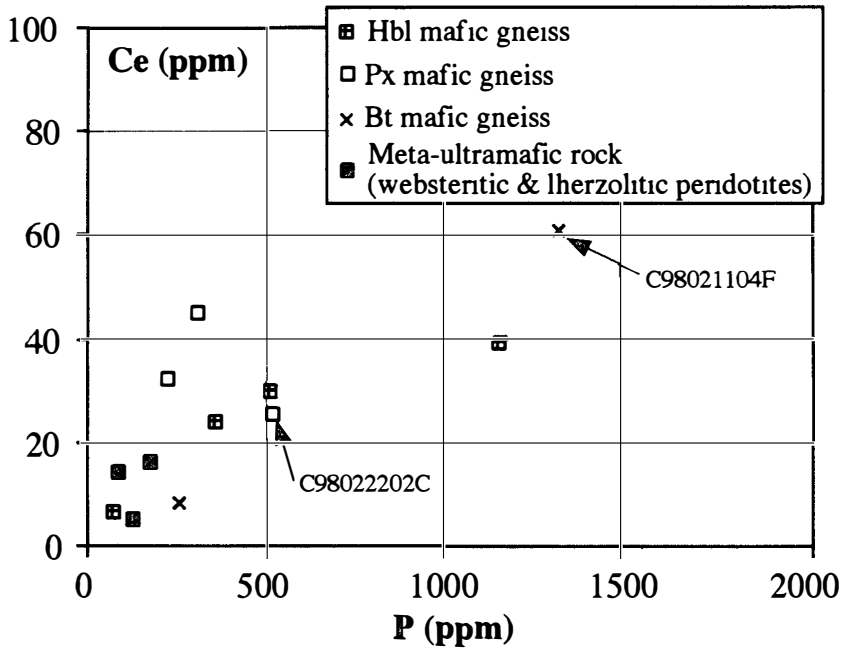

Fig 9 Ce (ppm)-P (ppm) diagram of the mafic gneisses and the meta-ultramafic rocks from Tonagh Island

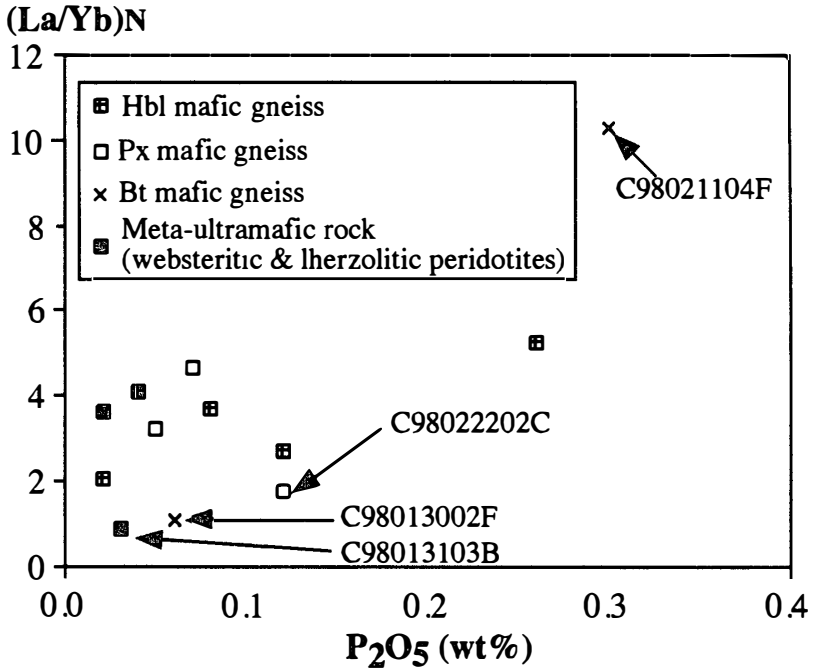

Fig 10 $(La/Yb)_N$-P_2O_5 wt% diagram of the mafic gneisses and the meta-ultramafic rocks from Tonagh Island

samples (C98013103B and C98013002F) show lower $(La/Yb)_N$ ratios than those of the LREE-enriched ones (Fig 10) These lines of evidence suggest that the LREE-enriched mafic gneisses and ultramafic rocks on Tonagh Island have been derived from LREE-enriched mantle rather than LREE flat ones.

Acknowledgments

We are grateful to Drs J-I Kimura and N Tsuchiya for critical reading and useful comments We would like to thank to Prof H Ishizuka for his constructive comments and discussion We are grateful to Profs T Kano, T Kawasaki and Dr S Suzuki for useful comments Thanks also go to Dr A Kamei, Mrs T Yamasaki, T Ando and Y Morifuku for their help in the chemical analyses

References

Black, L P, Williams, I S and Compston, W (1986) Four zircon ages from one rock the history of a 3930 Ma-old granulite from Mount Sones, Antarctica Contrib Mineral Petrol, **94**, 427-437

Cattell, A (1987) Enriched komatiitic basalts from Newton Township, Ontario their genesis by crustal contamination of depleted komatiite magma Geol Mag, **124**, 303-309

Harley, S L and Black, L P (1997) A revised Archaean geochronology for the Napier Complex, Enderby Land, from SHRIMP ion-microprobe studies Antarct Sci, **9**, 74-91

Harley, S L and Hensen, B J (1990) Archaean and Proterozoic high-grade terranes of East Antarctica (40-80°E) A case study of diversity in granulite facies metamorphism High-temperature metamorphism and crustal anatexis, ed by J R Ashworth and M Brown London, Unwin Hyman, 320-370

Hokada, T, Osanai, Y, Toyoshima, T, Owada, M, Tsunogae, T and Crowe, W A (1999) Petrology and metamorphism of sapphirine-bearing aluminous gneisses from Tonagh Island in the Napier Complex, Enderby Land, East Antarctica Polar Geosci, **12**, 1-28

Jahn, B, Gruau, G and Glikson, A Y (1982) Komatiites of the Onverwacht Group, S Africa REE geochemistry, Sm/Nd age and mantle evolution Contrib Mineral Petrol, **80**, 25-40

Kretz, R (1983) Symbols for rock-forming minerals Am Mineral, **68**, 277-279

Martin, H (1986) Effect of steeper Archaean geothermal gradient on geochemistry of subduction-zone magmas Geology, **14**, 753-756

Osanai, Y, Toyoshima, T, Owada, M, Tsunogae, T, Hokada, T and Crowe, W A (1999) Geology of the ultrahigh-temperature metamorphic rocks from Tonagh Island in the Napier Complex, Enderby Land, East Antarctica Polar Geosci, **12**, 1-28

Owada, M, Osanai, Y, Kagami, H and Shiraishi, K (1995) Isotopic re-equilibration of early to middle Archaean crust by late Archaean tectonothermal event in the Napier Complex, East Antarctica Abst VII Inter Symp Antarct Ear Sci, Siena, 292

Owada, M, Osanai, Y, Toyoshima, T, Tsunogae, T, Hokada, T and Crowe, W A (1999) Petrography and geochemistry of mafic and ultramafic rocks from Tonagh Island in the Napier Complex, East Antarctica A preliminary report Polar Geosci, **12**, 87-100

Sheraton, J W and Black, L P (1981) Geochemistry and geochronology of Proterozoic tholeiite dykes of East Antarctica Evidence for mantle metasomatism Contrib Mineral Petrol, **78**, 305-317

Sheraton, J W, Offe, L A, Tingey, R J and Ellis, D J (1980) Enderby Land, Antarctica—an usual Precambrian high-grade metamorphic terrain J Geol Soc Aust, **27**, 1-18

Sheraton, J W, Tingey, R J, Black, L P, Offe, L A and Ellis, D J (1987) Geology of Enderby Land and western Kemp Land, Antarctica BMR Bull, **223**, 51 p

Sun, S S and McDonough, W F (1989) Chemical and isotopic systematics of oceanic basalts Implications for mantle composition and processes Magmatism in the Ocean Basins, ed by A D Saunders and M J Norry Oxford, Blackwell, 313-345 (Geol Soc Spec Publ, No 42)

Sun, S S and Nesbitt, R W (1978) Petrogenesis of Archaean ultrabasic and basic volcanics Evidence from rare earth elements Contrib Mineral Petrol, **65**, 301-325

Suzuki, S, Hokada, T, Ishikawa, M and Ishizuka, H (1999) Geochemical study of granulites from Mt Riiser-Larsen, Enderby Land, East Antarctica Implication for protoliths of the Archaean Napier Complex Polar Geosci, **12**, 101-125

Tainosho, Y, Kagami, H, Hamamoto, T and Takahashi, Y (1997) Preliminary result for the Nd and Sr isotope characteristics of the Archaean gneisses from Mount Pardoe, Napier Complex, East Antarctica Proc NIPR Symp Antarct Geosci, **10**, 92-101

Toyoshima, T, Osanai, Y, Owada, M, Tsunogae, T, Hokada, T and Crowe, W A (1999) Deformation of ultrahigh-temperature metamorphic rocks from Tonagh Island in the Napier Complex, East Antarctica Polar Geosci, **12**, 29-48

Tribuzio, R, Tiepolo, M and Thirlwall, M (2000) Origin of titanian pargasite in gabbroic rocks from the Northern Apennine ophiolites (Italy) insights into the late-magmatic evolution of a MOR-type intrusive sequence Earth Planet Sci Lett, **176**, 281-293

Tsunogae, T, Osanai, Y, Toyoshima, T, Owada, M, Hokada, T and Crowe, W A (1999) Metamorphic reactions and preliminary *P-T* estimations of ultrahigh-temperature mafic granulite from Tonagh Island in the Napier Complex, East Antarctica Polar Geosci, **12**, 29-48

(Received March 24, 2000, Revised manuscript accepted June 14, 2000)

Appendix 1 Representative pyroxene analysis of the Hbl therzolitic peridotite

Mineral	Opx	Opx	Opx	Opx	Opx	Opx	Opx	Opx	Opx	Opx	Cpx	Cpx	Cpx
Analy No	1	2	3	5	6	7	9	10	11	12	4	8	13
	core	core	core	core	core	core	core	core	core	in Ol	core	core	in Ap
SiO_2	55 39	54 58	55 02	54 67	55 03	54 92	54 88	55 10	54 96	51 67	49 83	51 93	50 71
TiO_2	0 31	0 00	0 02	0 00	0 00	0 36	0 00	0 25	0 00	0 00	0 66	1 07	0 68
Al_2O_3	3 18	3 28	3 43	3 31	2 93	3 78	3 02	3 05	2 80	1 62	4 51	4 46	4 36
Cr_2O_3	0 00	0 31	0 01	0 19	0 19	0 20	0 00	0 20	0 00	0 00	0 11	0 06	0 23
FeO	11 47	10 83	10 34	11 35	11 13	11 37	10 97	10 88	11 52	12 40	5 92	3 83	3 19
MnO	0 12	0 12	0 00	0 00	0 00	0 23	0 11	0 00	0 10	0 00	0 17	0 00	0 11
MgO	29 88	29 70	29 77	30 06	30 56	29 22	30 71	29 98	29 72	33 83	16 12	15 36	15 24
CaO	0 26	0 47	0 82	0 26	0 23	0 09	0 29	0 32	0 36	0 12	21 56	23 04	23 75
Na_2O	0 04	0 21	0 06	0 00	0 00	0 02	0 13	0 02	0 22	0 03	0 62	0 60	0 56
K_2O	0 00	0 06	0 00	0 03	0 19	0 00	0 06	0 11	0 00	0 00	0 21	0 16	0 16
Total	100 65	99 56	99 47	99 87	100 26	100 19	100 17	99 91	99 68	99 67	99 71	100 51	98 99
O	6	6	6	6	6	6	6	6	6	6	6	6	6
Si	1 939	1 932	1 941	1 929	1 934	1 931	1 930	1 940	1 946	1 855	1 849	1 890	1 878
Ti	0 008	0 000	0 001	0 000	0 000	0 010	0 000	0 007	0 000	0 000	0 018	0 029	0 019
Al	0 131	0 137	0 143	0 138	0 121	0 157	0 125	0 127	0 117	0 069	0 197	0 191	0 190
Cr	0 000	0 009	0 000	0 005	0 005	0 006	0 000	0 006	0 000	0 000	0 003	0 002	0 007
Fe	0 336	0 321	0 305	0 335	0 327	0 334	0 323	0 320	0 341	0 372	0 184	0 117	0 099
Mn	0 004	0 004	0 000	0 000	0 000	0 007	0 003	0 000	0 003	0 000	0 005	0 000	0 003
Mg	1 559	1 567	1 565	1 581	1 601	1 531	1 610	1 573	1 568	1 810	0 891	0 833	0 841
Ca	0 010	0 018	0 031	0 010	0 009	0 003	0 011	0 012	0 014	0 005	0 857	0 898	0 943
Na	0 003	0 014	0 004	0 000	0 000	0 001	0 009	0 001	0 015	0 002	0 045	0 042	0 040
K	0 000	0 003	0 000	0 001	0 009	0 000	0 003	0 005	0 000	0 000	0 010	0 007	0 008

Total Fe as FeO

Electron microprobe analyzer (JOEL JED-2140) at Okayama University determined mineral chemistry The data were obtained under conditions of 15 kV accelerating voltage